

Submicron Scale-Structured Hydrophilic Titanium Surfaces Promote Early Osteogenic Gene Response for Cell Adhesion and Cell Differentiation

Marcus Oliver Klein, PD, Dr. med., Dr. med. dent.;* Ana Bijelic, Dr. med. dent.;[†]
Thomas Ziebart, Dr. med, Dr. med. dent., Dr. rer. Nat.;[‡] Felix Koch, Dr. med., Dr. med. dent.;[§]
Peer W. Kämmerer, Dr. med., Dr. med. dent.;[¶] Marco Wieland, Ph.D.;**
Moritz A. Konerding, Prof., Dr. med.;^{††} Bilal Al-Nawas, Prof., Dr. med., Dr. med. dent.^{‡‡}

ABSTRACT

Background and Purpose: Titanium (Ti) surface roughness and surface hydrophilicity are key factors to regulate osteogenic cell responses during dental implant healing. In detail, specific integrin-mediated interactions with the extracellular environment trigger relevant osteogenic cell responses like differentiation and matrix synthesis via transcriptions factors. Aim of this study was to monitor surface-dependent osteogenic cell adhesion dynamics, proliferation, and specific osteogenic cell differentiation over a period of 7 days.

Materials and Methods: Ti disks were manufactured to present smooth pretreatment (PT) surfaces and rough sandblasted/acid-etched (SLA) surfaces. Further processing to isolate the uncontaminated TiO₂ surface from contact with atmosphere provided a highly hydrophilic surface without alteration of the surface topography (modSLA). Tissue culture polystyrene (TCPS) served as control. Human osteogenic cells were cultivated on the respective substrates. After 24 hours, 48 hours, 72 hours, and 7 days, cell morphology on the Ti substrates was visualized by scanning transmission electron microscopy. As a marker of cellular proliferation, cell count was assessed. For the analysis of cell adhesion and differentiation, specific gene expression levels of the integrin subunits $\beta 1$ and αv , runx-2, collagen type I α (COL), alkaline phosphatase (AP), and osteocalcin (OC) were obtained by real-time RT-PCR for the respective time points. Data were normalized to internal controls.

Results: TCPS and PT surfaces preserved a rather immature, dividing osteogenic phenotype (high proliferation rates, low integrin levels, and low specific osteogenic cell differentiation). SLA and especially modSLA surfaces promoted both cell adhesion as well as the maturation of osteogenic precursors into post-mitotic osteoblasts. In detail, during the first 48 hours, modSLA resulted in lowest cell proliferation rates but exhibited highest levels of the investigated integrins, runx-2, COL, AP, and OC.

Conclusion: Our results revealed a strong synergistic effect between submicron-scale roughness and surface hydrophilicity on early osteogenic cell adhesion and maturation.

KEY WORDS: cell adhesion, cell differentiation, integrins, osteocalcin, osteogenic cell proliferation, runx-2, surface hydrophilicity, titanium surface modifications

*Specialist for oral and maxillofacial surgery, Oral and Maxillofacial Surgery, University Medicine Mainz, Mainz, Germany; [†]dentist, Oral and Maxillofacial Surgery, University Medicine Mainz, Mainz, Germany; [‡]scientific associate and trainee for oral and maxillofacial surgery, Oral and Maxillofacial Surgery, University Medicine Mainz, Mainz, Germany; [§]specialist for oral and maxillofacial surgery, Oral and Maxillofacial Surgery, University Medicine Mainz, Mainz, Germany; [¶]scientific associate and trainee for oral and maxillofacial surgery, Oral and Maxillofacial Surgery, University Medicine Mainz, Mainz, Germany; **management, MyoPowers Medical Technologies SA, Lausanne, Switzerland; ^{††}associate professor, Department of Anatomy, Johannes Gutenberg-University Mainz, Mainz, Germany;

^{‡‡}associate professor, specialist for oral and maxillofacial surgery, Oral and Maxillofacial Surgery, University Medicine Mainz, Mainz, Germany

Reprint requests: PD Dr. med. Dr. med. dent. Marcus Oliver Klein, Department of Oral and Maxillofacial Surgery, University Medicine Mainz, Augustusplatz 2, 55131 Mainz, Germany; e-mail: klein@mkg.klinik.uni-mainz.de

© 2011 Wiley Periodicals, Inc.

DOI 10.1111/j.1708-8208.2011.00339.x

INTRODUCTION

In modern dental implantology, one key task is to enhance the implant healing cascade in order to achieve early and stable osseointegration. Accordingly, innovative surface modifications aim to promote respective responses of surrounding osteogenic host cell populations. Up to now, because of its high biocompatibility and promising physicochemical properties, titanium (Ti) is a very favorable substrate to develop and test surface modifications.^{1–3} Generally, Ti surface modifications are addressed to topographical properties and chemical composition.

Well-established methods for ablative roughening of implant surfaces are sandblasting and acid etching. Although sandblasting of Ti substrates produces micron scale roughness, acid-etching or combination of the two methods (SLA: sandblasted, acid-etched) even results in submicron scale topography.⁴ Recent *in vitro* studies have shown the impact of these topographic surface modifications on osteogenic cell attachment, spreading, gene expression, and cytokine release^{1,5,6} but in most cases only for selected time points or over a short period of time.

Another material property that can influence cell behavior is surface hydrophilicity.⁷ One approach to obtain hydrophilic, highly energetic surface is to isolate the uncontaminated (titanium dioxide) TiO₂ surface from contact with atmosphere. Compared with conventional SLA surfaces, these modified surfaces (modSLA) have been proven to enhance protein adsorption⁸ and to promote a differentiated osteogenic phenotype, whereas cell proliferation decreased.⁷ These *in vitro* findings – however on short time periods not more than a few days – are consistent with animal studies showing improved soft tissue and hard tissue integration and mechanical stability for dental implants initially presenting hydrophilic surface properties^{9–12} as well as with clinical observations indicating enhanced implant stability.¹³

Like for all mesenchymal cells, sufficient osteogenic cell adhesion to the biomaterial is mandatory precondition for further cellular proliferation, differentiation, and matrix synthesis. Whereas initial cell attachment is based on rather unspecific cell-substrate interactions, true cell adhesion displays complex interactions between extracellular ligands and specific cellular receptors with high impact on further intracellular signal transduction.¹⁴ Integrin receptors are transmembrane heterodimers consisting of non-covalently associated α

and β subunits. The subunits β_1 and α_v have affinity to extracellular matrix proteins like fibronectin, collagen (COL), and osteonectin via the RGD tripeptide sequence.¹⁵ Integrin-mediated outside-in-signalling has been shown to regulate osteogenic cytoskeleton organization and gene expression.^{15,16} Furthermore, during osteoblast/substrate interactions, the expression of these adhesion molecules is modified according to distinct surface characteristics.¹⁵

The osteoblastic lineage is characterized by a defined sequence of proliferation and maturation stages. Although immature osteoprogenitor cells show a comparable high proliferative activity, cell proliferation decreases in subsequent maturation stages up to post-mitotic mature osteoblasts.^{17,18} A variety of respective “phenotypic genes” have been identified with COL and alkaline phosphatase (AP) expressed during early osteogenic differentiation, followed by subsequent transcription of non-collagenous bone matrix proteins like osteopontin (OPN) and finally osteocalcin (OC).¹⁹

Specific transcription factors have been shown to direct immature marrow stromal cells toward mature osteoblasts. Runt-related gene 2 (*runx-2*) has been identified as an essential transcription factor for osteogenic cell differentiation with “sequential” expression of the *runx-2*-regulated phenotypic genes like COL, ALP, OPN and OC.^{20–22}

Aim of the study was to monitor osteogenic cell morphology and proliferation dynamics as well as specific gene expression levels for cell adhesion and *runx-2*-related cell differentiation on (1) rather smooth, (2) submicron scale structured, and (3) additionally modified hydrophilic Ti surfaces over a time period of 7 days.

MATERIALS AND METHODS

Substrates

Surface-modified Ti disks were supplied by the Institut Straumann (Basel, Switzerland). One-millimeter-thick sheets of grade 2 unalloyed Ti (ASTM F67 “Unalloyed Ti for surgical implant applications”) were punched to 15 mm in diameter. The methods used to prepare SLA and modSLA surfaces out of smooth pretreatment (PT) Ti disks have been reported previously.⁷

Prior to use, PT and SLA disks were washed, sonicated, and sterilized in an oxygen plasma cleaner (PDC-32G, Harrick Plasma, Ithaca, NY, USA). The modSLA disks were produced by rinsing SLA disks under

nitrogen protection to prevent exposure to atmosphere during processing, and then stored in a sealed glass tube under nitrogen-containing isotonic NaCl solution, followed by gamma irradiation (25 kGy) over night for sterilization. These procedures did not alter surface topography or roughness parameters. Recent topographic investigations revealed a mean peak to valley roughness (R_a) of 40 nm for the smooth PT surface and identical R_a values of 3.2 μm for the SLA and modSLA surfaces, respectively. In contrast to the PT and SLA surfaces, modSLA processing resulted in significantly less carbon contamination and an extremely hydrophilic surface.^{3,4,7} Tissue culture polystyrene (TCPS) served as a control group.

Cell Culture

A commercial hipbone-derived osteoblastic cell line, human osteoblasts (PromoCell, Heidelberg, Germany) was cultivated on TCPS using standard osteoblast cultivation medium, consisting of fetal calf serum (Gibco Invitrogen, Darmstadt, Germany), Dulbecco's modified Eagle's medium (D-MEM, Gibco Invitrogen), dexamethasone (100 nmol/L, Serva Bioproducts, Heidelberg, Germany), L-glutamin (Gibco Invitrogen), and streptomycin (100 $\mu\text{g}/\text{mL}$, Gibco Invitrogen). Cells were passaged at regular intervals depending on their growth characteristics using 0.5% trypsin (Seromed Biochrom KG, Berlin, Germany). For the experiments, a defined number of cells (45.000/ cm^2) out of the fourth passage were applied to the respective substrates (TCPS, PT, SLA, modSLA), using the same cultivation medium. Cultivation was proceeded at 37°C in a constant humidified atmosphere of 95% air and 5% CO_2 .

Cell count and reverse transcription polymerase chain reaction (RT-PCR) experiments were carried out after 24 hours, 48 hours, 72 hours, and 7 days. Cells were released from the surface by incubation with 0.5% trypsin with ethylenediaminetetraacetic acid for 5 minutes, followed by gentle tapping to remove remaining cells. The reaction was stopped by adding culture medium, followed by two steps of centrifugation to remove remaining trypsin out of the cell suspension.

RNA Isolation

After detaching the cells from the respective surfaces, cells were transferred into a tube and recentrifuged for 5 minutes at 1.800 rpm. Total RNA was isolated using the RNeasy kit (Qiagen, Hilden, Germany) following

the manufacturer's instructions. Cell pellets were lysed by addition of 350 μL Qiagen Buffer RLT and β -mercaptoethanol. Cell lysates were transferred into the QIAshredder and homogenized by centrifugation at 13.000 rpm for 2 minutes. After addition of 350 μL of 70% ethanol, the homogenized lysate was applied to an RNeasy spin column placed in a 15 mL centrifuge tube and centrifuged for 15 seconds at 10.000 rpm. After addition of 350 μL Qiagen Buffer RW1 with subsequent centrifugation for 15 seconds at 10.000 rpm, RNase-free DNase set (Qiagen, Hilden, Germany) was added for 15 minutes to avoid DNA-contamination, followed by addition of Buffer RW1 and centrifugation. Columns were washed twice in 500 μL Buffer RPE at 10.000 rpm for 15 seconds and 2 minutes, respectively. Subsequently, the isolated RNA was eluted in 50 μL of RNase-free water and stored at -20°C until photometric measurement.

Photometric RNA Measurement

Concentration of the isolated RNA was assessed by the NanoDrop spectrophotometer (peqLab, Erlangen, Germany). RNA concentration was adjusted to 25 ng/ μL .

Quantitative Real-Time RT-PCR

PCR was carried out using a 25 μL final reaction volume containing of 1.0 μL isolated RNA (concentration: 25 ng/ μL), 7.0 μL H_2O , 13.0 μL one-step SYBR Green RT-PCR mix (Bio-Rad, Hercules, USA) and 4 μL of primer (sense and antisense, concentration: 20 pg/ mL) employing the MJ MiniOpticon Real Time PCR-System (Bio-Rad, Hercules, USA). The one-step RT-PCR mix already contained all necessary reagents both for reverse transcription and for polymerase chain reaction like reverse transcriptase, heat stable DNA-polymerase, nucleotids, the fluorescent dye SYBR Green I as well as an optimized buffer. The oligonucleotides used as primers (synthesized by MWG-Biotech AG, Ebersberg, Germany) are summarized in Table 1. The RNA was reverse transcribed into cDNA at 50°C for 10 minutes, followed by inactivation of the reverse transcriptase at 95°C for 5 minutes. Then, the targets were amplified by multiplex (40 cycles) PCR with thermal cycling parameters of 56°C for 30 seconds (primer annealing), 72°C for 30 seconds (complementary strand synthesis), fluorescence signal reading, and 95°C for 10 seconds (DNA denaturation). For each investigated surface and time point, assays were run in triplicate. According to the method of Pfaffl,²³ transcription levels of the

TABLE 1 Oligonucleotide Primer Sequences for the Real-Time Reverse Transcription Polymerase Chain Reaction. The Accession Numbers Refer to Gene-Database "Nucleotide" of the National Center for Biotechnology Information (<http://www.ncbi.nlm.nih.gov/>).

Gene	Accession Number	Primer Sequence	Amplicon Size (bp)
Integrin β_1	NM_002211	sense: agt ttg ctg tgt gtt tgc tc antisense: gcc tct ggg att ttc tat gt	214 bp
Integrin α_v	NM_002210	sense: ttg ttt cag gag ttc caa ga antisense: tga aga gag gtg ctc caa ta	186 bp
Runx-2	NM_004348	sense: ccc acg aat gca cta tcc antisense: gga cat acc gag gga cat	37 bp
Collagen I α	NM_000088	sense: aga act ggt aca tca gca ag antisense: gag ttt aca gga agc aga c.	431 bp
Alkaline Phosphatase	NM_000478	sense: tac gag ctg aac agg aac aa antisense: ctt ctt gtc tgt gtc act c.	296 bp
Osteocalcin	NM_199173	sense: gca aag gtg cag cct ttg tg antisense: ggc tcc cag cca ttg ata cag	45 bp
β -Actin	NM_001101	sense: gga gca atg atc ttg atc tt antisense: cct tcc tgg gca tgg agt cct	204 bp
GAPDH	NM_002046	sense: aaa aac ctg cca aat atg at antisense: cag tga ggg tct ctc tct tc	277 bp

BP = base pair; GAPDH = glycerin-aldehyd-3-phosphat-dehydrogenase; runx-2 = runt-related gene 2.

investigated genes of interest were normalized to those of two housekeeping genes.^{24,25} In a preliminary investigation, the housekeeping genes *β -actin* and *glycerin-aldehyd-3-phosphat-dehydrogenase* (*GAPDH*) were identified as suitable for the investigated surfaces and cell line by employing the software *geNorm* (<http://www.medgen.ugent.be/~jvdesomp/genorm/>).²⁶

Assessment of Osteogenic Cell Morphology: Scanning Transmission Electron Microscopy (STEM) Studies

STEM was employed to visualize osteogenic cell morphology on the different Ti surfaces for the respective time points (24 hours, 48 hours, 72 hours, and 7 days). In brief, cells were prepared as follows: cells were fixed in 1.5% paraformaldehyde/1.5% glutaraldehyde in phosphate buffer for 2 hours and post-fixed in 1.0% osmium tetroxide/1.5% ferricyanide for 2 hours, followed by dehydration by an ethanol gradient and embedded in *Lemix Epoxy Resin* (TAAB Laboratories Equipment Ltd, Aldermaston, UK). Ultrathin sections (60–90 nm) were stained with uranyl acetate and *Reynold's lead citrate*.²⁷ Images were acquired using a FEI/Philips CM120 transmission electron microscope (FEI Europe, Eindhoven, Netherlands).

Statistical Analysis

For each tested surface and given time point, three assays were run for the assessment of the cell number as well as for the assessment of gene expression via real-time RT-PCR, leading to independent data for the respective time points. Because of the small sample size, only descriptive statistical methods were applied. Results were shown in vertical bar charts (mean values with standard deviations).

RESULTS

Osteogenic Cell Morphology

In general, the smooth PT surface (R_a 40 nm) resulted in a larger and more flattened osteogenic phenotype, compared with the rough SLA and modSLA surfaces (R_a 3.2 μ m). After 24 hours, cells on all three Ti surfaces were well attached with a flat morphology and development of lamellipodia (PT > SLA > modSLA). Whereas the SLA surface showed more elongated cells, the modSLA surface exhibited rather roundish, small cells. After 48 hours and 72 hours, cell number increased for all three surfaces (PT = SLA > modSLA) with cell accumulation especially on the SLA and modSLA surfaces.

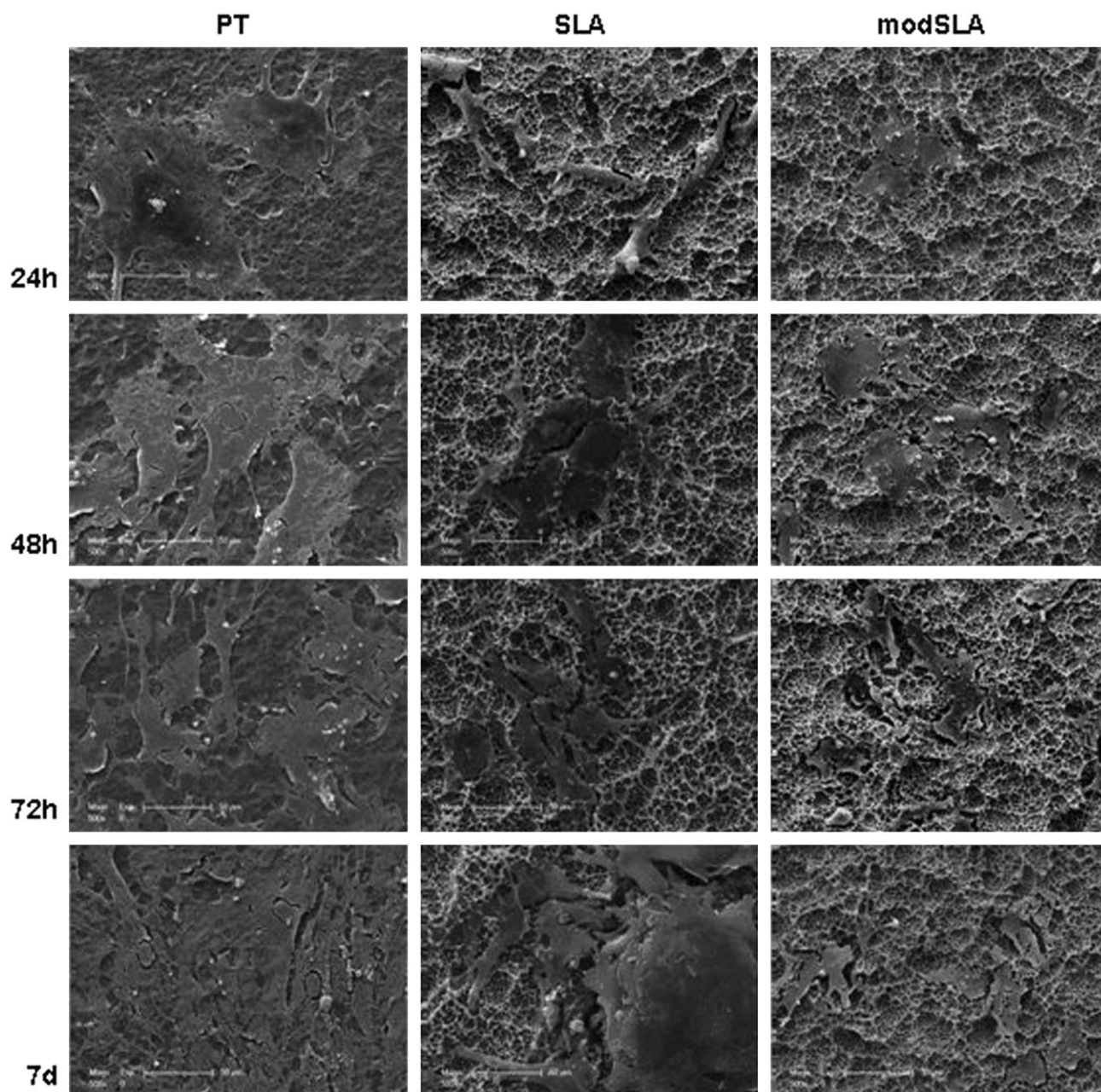


Figure 1 Representative scanning transmission electron microscopy images of osteogenic cells cultivated on the different titanium surface modifications (500-fold magnification).

For the rough SLA and modSLA surfaces, cell parts like lamellipodia bridging the surface pits were frequently observed. After 7 days, both for the PT surface as well as for the SLA surface, a significant increased cell number was observed, leading to an almost confluent cell layer on the PT surface. For the modSLA surface, multiple small cell nests were observed (Figure 1).

Cell Adhesion

Besides descriptive scanning electron microscopy to monitor osteogenic cell attachment, cell adhesion

dynamics were quantified by assessment of gene expression levels of the integrin β_1 and integrin α_v subunits. For the modSLA surface, integrin β_1 expression was moderately enhanced after 24 hours and strongly enhanced after 48 hours, compared with the other surfaces (TCPS, PT, SLA) that showed almost identical expression levels during the whole observation period (Figure 2). For the modSLA surface, integrin α_v expression was strongly enhanced after 24 hours and 48 hours, compared with the other surfaces. After 24 hours, the SLA surface resulted in moderately enhanced expression

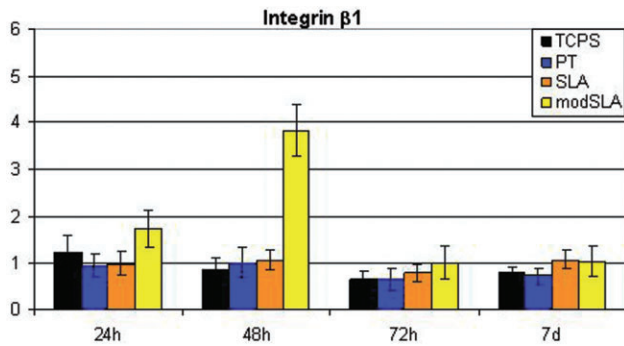


Figure 2 Integrin β_1 gene expression levels for the respective surfaces and investigated time points, normalized to the internal controls β -actin and GAPDH (mean values out of triplets, error bars: standard deviations). GAPDH = glycerin-aldehyd-3-phosphat-dehydrogenase; PT = pretreatment; TCPS = tissue culture polystyrene.

levels, compared with the TCPS and PT surfaces; after 72 hours, integrin α_v expression was slightly enhanced on the SLA surface, compared with the other surfaces (TCPS, PT, modSLA; Figure 3).

Cell Proliferation

All investigated surfaces promoted continuous cell growth over 7 days (Figure 4). Whereas basically no differences of the cell numbers for the TCPS, PT, and SLA surfaces could be observed, the modSLA surface resulted in lowest cell proliferation.

Cell Differentiation

For the modSLA surface, gene expression of the transcription factor runx-2 was strongly enhanced after 24 hours and 48 hours and moderately enhanced after 72

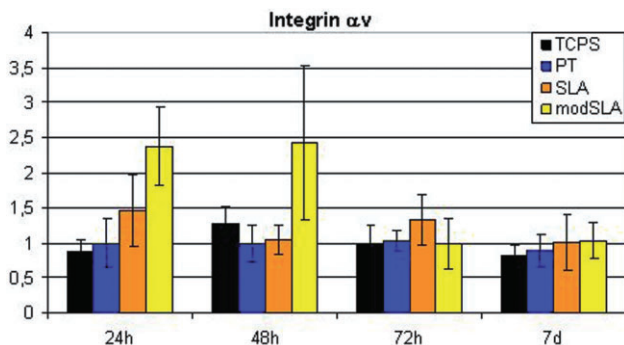


Figure 3 Integrin α_v gene expression levels for the respective surfaces and investigated time points, normalized to the internal controls β -actin and GAPDH (mean values out of triplets, error bars: standard deviations). GAPDH = glycerin-aldehyd-3-phosphat-dehydrogenase; PT = pretreatment; TCPS = tissue culture polystyrene.

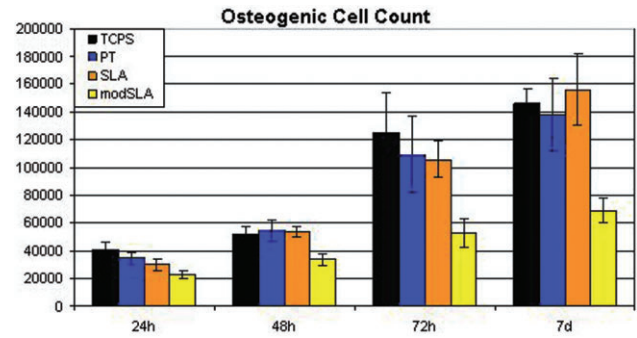


Figure 4 Cell counts for the respective surfaces and investigated time points (mean values out of triplets, error bars: standard deviations). PT = pretreatment; TCPS = tissue culture polystyrene.

hours, compared with all other surfaces. For the SLA surface, runx-2 expression was enhanced after 24 hours, compared with the TCPS and PT surfaces (Figure 5). The early differentiation markers COL type I α and AP showed almost identical gene expression profiles: after 24 hours, a strongly enhanced expression could be detected for the modSLA surface, compared with all other surfaces. For the SLA surface, an enhanced COL and AP expression compared with the TCPS and PT surfaces could be detected as well after 24 hours. After 48 hours, expression of COL and AP was still moderately increased for the modSLA surface, compared with all other surfaces. After 72 hours, COL and AP expression was slightly increased for the SLA surface, compared with the modSLA surface and stronger increased compared with the TCPS and PT surfaces (Figures 6 and 7). For the modSLA surface, gene expression of the late differentiation marker OC was strongly increased after

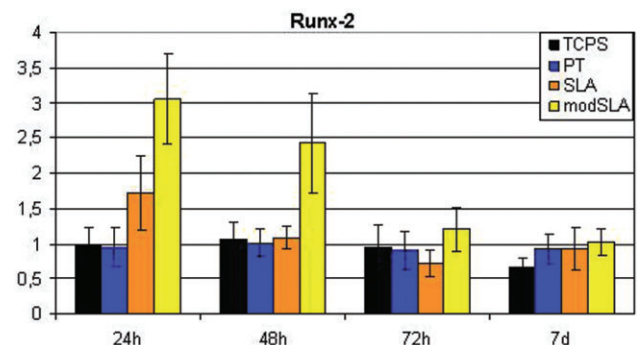


Figure 5 Runx-2 gene expression levels for the respective surfaces and investigated time points, normalized to the internal controls β -actin and GAPDH (mean values out of triplets, error bars: standard deviations). PT = pretreatment; TCPS = tissue culture polystyrene.

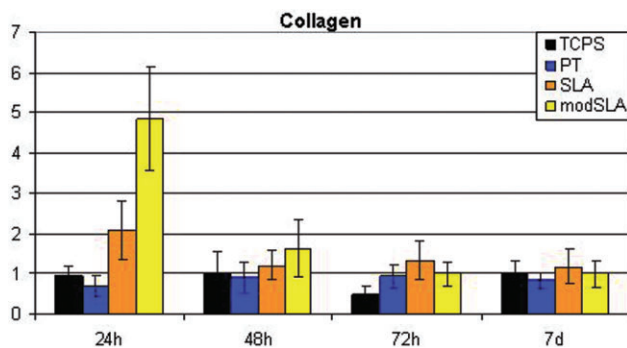


Figure 6 Collagen type Iα gene expression levels for the respective surfaces and investigated time points, normalized to the internal controls β-actin and GAPDH (mean values out of triplets, error bars: standard deviations). GAPDH = glycerin-aldehyd-3-phosphat-dehydrogenase; PT = pretreatment; TCPS = tissue culture polystyrene.

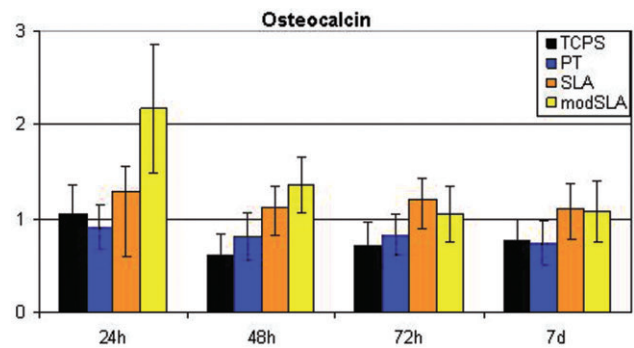


Figure 8 Osteocalcin gene expression levels for the respective surfaces and investigated time points, normalized to the internal controls β-actin and GAPDH (mean values out of triplets, error bars: standard deviations). GAPDH = glycerin-aldehyd-3-phosphat-dehydrogenase; PT = pretreatment; TCPS = tissue culture polystyrene.

24 hours compared with the other surfaces. After 24 hours, OC expression was slightly increased for the SLA surface, compared with the TCPS and PT surfaces. After 48 hours, for the modSLA surface, OC expression was slightly increased compared with the SLA surface and strongly increased compared with the TCPS and PT surfaces. After 48 hours, for the SLA surface, OC expression was slightly increased compared with the PT surface and strongly increased compared with the TCPS surface. After 72 hours and 7 days, for the SLA and modSLA surfaces, OC expression was moderately increased compared with the TCPS and PT surfaces (Figure 8).

DISCUSSION

Today, the insertion of endosseous dental implants has become a major treatment alternative for the functional

rehabilitation of fully or partly edentulous jaws. Promising long-term results for well-established treatment sites with optimum bone quality, such as the interforaminal region of the lower jaw,²⁸ have led to a continuous expansion of indications and introduction of more offensive treatment protocols like implantation into augmented areas, immediate implantation following tooth extraction and/or immediate loading of dental implants.^{29–32} Furthermore, patients with limitations of tissue homeostasis and integrity like after radiation therapy to the head and neck region or with impaired bone remodeling and repair capacity because of metabolic disorders or systemic medication (e.g., bisphosphonates) have been identified as challenging collectives for the treatment with dental implants.^{33,34}

Accordingly, modern Ti implant surfaces have to meet the requirements of high biocompatibility with optimal responses of adjacent osteogenic cell populations. Especially surface modifications like (micro-) roughness and enhanced free surface energy are in the focus of scientific interest. Aim of the present study was to monitor the relevant osteogenic cell attributes *adhesion*, *proliferation*, and *differentiation* on, respectively, surface modified titanium substrates over a comparable long period of time (7 days).

As already stated in the introduction, *specific* integrin-mediated osteogenic cell adhesion serves as indispensable precondition for subsequent cellular attributes like proliferation and differentiation.¹⁴ Furthermore, for osteogenic cells, the integrin subunits β₁ and α_v have been shown to trigger effects of cytokines like bone morphogenetic protein 2.³⁵ In our study, the

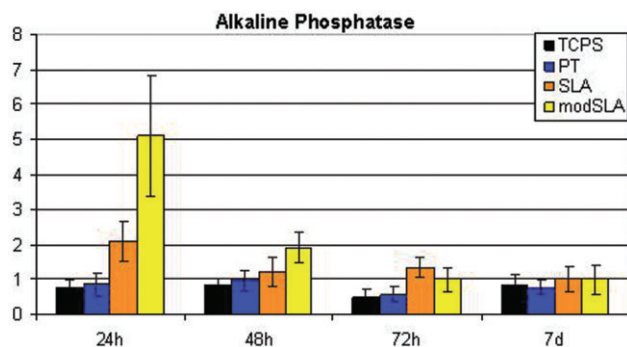


Figure 7 Alkaline phosphatase gene expression levels for the respective surfaces and investigated time points, normalized to the internal controls β-actin and GAPDH (mean values out of triplets, error bars: standard deviations). GAPDH = glycerin-aldehyd-3-phosphat-dehydrogenase; PT = pretreatment; TCPS = tissue culture polystyrene.

hydrophilic modSLA surface resulted in markedly increased gene expression levels of these integrin subunits during the first 48 hours, thus arranging the cells for respective differentiation stimuli.

In contrast, cell proliferation was lowest for the modSLA surface with approximately half the cell count at the end of the observation period, compared with the other investigated surfaces. These results are consistent with those of Zhao and colleagues, who indicated a reverse relation between surface hydrophilicity and initial cell proliferation.^{3,7} At the end of the observation period, our scanning electron microscopy studies identified almost confluent cell layers of comparable large-sized cells for the PT surface, whereas especially the modSLA surface resulted in multiple non-confluent aggregates of rather small osteogenic cells.

In accordance with Liu and colleagues,¹⁹ we investigated the runx-2-dependent early osteogenic differentiation markers COL type I α and AP as well as the late differentiation marker OC, whose expression is also highly controlled by runx-2 levels.²² In bony tissue, COL plays a pivotal role both for overall mechanical stability as well as for osteogenic cell adhesion, proliferation, and further differentiation.³⁶ AP plays an important regulatory role during matrix mineralization.^{37,38} OC, which is only synthesized by mature osteoblasts, is directly associated with bone matrix mineralization as well.^{39,40} Our results revealed enhanced expression levels of the transcription factor runx-2 as well as for the differentiation markers COL, AP, and OC especially for the modSLA surface, followed by the SLA surface. Interestingly, an explicit increase (of the RNA levels) of these markers could be detected only during the first 48 hours with subsequent adaptation to the values of the TCPS and PT surfaces until day 7. For the interpretation of mRNA expression levels, it has to be kept in mind that varying mRNA translation and degradation kinetics as well as post-transcriptional mRNA modifications could result in differing protein levels.⁴¹ As a consequence, additional long-term monitoring of respective protein levels would be of great interest as well.

However, our results indicate a synergistic effect between submicron-scale roughness and surface hydrophilicity on early osteogenic cell adhesion and differentiation. In general, during the first 48 hours, the SLA surface promoted cell adhesion and differentiation more than the smooth PT surface. This effect was potentiated

by additional hydrophilic surface modifications (modSLA).

In a recent animal study, Omar and colleagues assessed early in vivo gene expression of peri-implant bone tissue via quantitative PCR both for anodically oxidized and for machined titanium implants.^{42,43} Within the first 24 hours, they found higher levels of the integrin subunits β_1 and α_v on the anodically oxidized Ti surface.⁴² After several days, they found significant higher AP levels (after 3 and 6 days) as well as higher OC levels (after 6 days) for the anodically oxidized Ti surface. Furthermore, the oxidized Ti surface revealed a higher amount of mesenchymal-like cells.⁴³ Except the cell count, these in vivo findings stand in line with our own in vitro results for the SLA and especially modSLA surface, indicating rapid recruitment, adhesion, and osteogenic cell differentiation for activated, highly biocompatible Ti surfaces.

Under physiological conditions, the osteogenic cell population forms a rather heterogeneous collective with a majority of immature and inactive progenitors that bear the potential to differentiate into mature osteoblasts – in case of appropriate stimuli like during normal bone remodeling or fracture repair. Thereby, these immature cells pass the stages of extensive proliferation, limited proliferation, and post-mitotic matrix synthesis.^{17,44} Our results indicate that the TCPS and PT surfaces tend to preserve a rather immature, dividing osteogenic phenotype, whereas SLA and especially hydrophilic modSLA surfaces seem to promote the maturation of osteogenic precursors into post-mitotic osteoblasts.

CONCLUSION

In summary, our study highlights the potential of Ti surface modifications to promote the healing of dental endosseous implants. Specific integrin-mediated interactions with the extracellular environment trigger consecutive intracellular signal transduction and relevant osteogenic cell responses like differentiation and matrix synthesis. The combination of submicron scale roughness and hydrophilicity synergistically promotes osteogenic cell adhesion and maturation in order to enhance implant healing also in compromised host tissues.

REFERENCES

1. Boyan BD, Lossdorfer S, Wang L, Zhao G, Lohmann CH, Cochran DL, Schwartz Z. Osteoblasts generate an osteogenic

- microenvironment when grown on surfaces with rough microtopographies. *Eur Cell Mater* 2003; 6:22–27.
2. Puleo DA, Nanci A. Understanding and controlling the bone-implant interface. *Biomaterials* 1999; 20:2311–2321.
3. Zhao G, Raines AL, Wieland M, Schwartz Z, Boyan BD. Requirement for both micron- and submicron scale structure for synergistic responses of osteoblasts to substrate surface energy and topography. *Biomaterials* 2007; 28:2821–2829.
4. Schlegel KA, Thorwarth M, Plesinac A, Wiltfang J, Rupprecht S. Expression of bone matrix proteins during the osseous healing of topical conditioned implants: an experimental study. *Clin Oral Implants Res* 2006; 17:666–672.
5. Zhao G, Zinger O, Schwartz Z, Wieland M, Landolt D, Boyan BD. Osteoblast-like cells are sensitive to submicron-scale surface structure. *Clin Oral Implants Res* 2006; 17:258–264.
6. Zinger O, Zhao G, Schwartz Z, Simpson J, Wieland M, Landolt D, Boyan B. Differential regulation of osteoblasts by substrate microstructural features. *Biomaterials* 2005; 26:1837–1847.
7. Zhao G, Schwartz Z, Wieland M, Rupp F, Geis-Gerstorfer J, Cochran DL, Boyan BD. High surface energy enhances cell response to titanium substrate microstructure. *J Biomed Mater Res A* 2005; 74:49–58.
8. Scheideler L, Rupp F, Wieland M, Geis-Gerstorfer J. Storage conditions of titanium implants influence molecular and cellular interactions. *Int Assoc Dent Res (IADR) 83rd General Session, Baltimore, MD, March 9–12, 2005. J Dent Res* 2005; 84(Spec Iss A). Abstract 870.
9. Buser D, Broggini N, Wieland M, et al. Enhanced bone apposition to a chemically modified SLA titanium surface. *J Dent Res* 2004; 83:529–533.
10. Kaback LA, Soung Do Y, Naik A, Smith N, Schwarz EM, O'Keefe RJ, Drissi H. Osterix/Sp7 regulates mesenchymal stem cell mediated endochondral ossification. *J Cell Physiol* 2008; 214:173–182.
11. Schwarz F, Herten M, Wieland M, Dard M, Becker J. [Chemically modified, ultra-hydrophilic titanium implant surfaces]. *Mund Kiefer Gesichtschir* 2007; 11:11–17.
12. Ferguson SJ, Broggini N, Wieland M, et al. Biomechanical evaluation of the interfacial strength of a chemically modified sandblasted and acid-etched titanium surface. *J Biomed Mater Res A* 2006; 78:291–297.
13. Oates TW, Valderrama P, Bischof M, et al. Enhanced implant stability with a chemically modified SLA surface: a randomized pilot study. *Int J Oral Maxillofac Implants* 2007; 22:755–760.
14. Keselowsky BG, Wang L, Schwartz Z, Garcia AJ, Boyan BD. Integrin alpha(5) controls osteoblastic proliferation and differentiation responses to titanium substrates presenting different roughness characteristics in a roughness independent manner. *J Biomed Mater Res A* 2007; 80:700–710.
15. Anselme K. Osteoblast adhesion on biomaterials. *Biomaterials* 2000; 21:667–681.
16. El-Ghannam AR, Ducheyne P, Risbud M, et al. Model surfaces engineered with nanoscale roughness and RGD tripeptides promote osteoblast activity. *J Biomed Mater Res A* 2004; 68:615–627.
17. Aubin JE. Advances in the osteoblast lineage. *Biochem Cell Biol* 1998; 76:899–910.
18. Malaval L, Liu F, Roche P, Aubin JE. Kinetics of osteoprogenitor proliferation and osteoblast differentiation in vitro. *J Cell Biochem* 1999; 74:616–627.
19. Liu F, Malaval L, Aubin JE. Global amplification polymerase chain reaction reveals novel transitional stages during osteoprogenitor differentiation. *J Cell Sci* 2003; 116(Pt 9): 1787–1796.
20. Ducy P, Zhang R, Geoffroy V, Ridall AL, Karsenty G. *Osf2/Cbfa1*: a transcriptional activator of osteoblast differentiation. *Cell* 1997; 89:747–754.
21. Qi H, Aguiar DJ, Williams SM, La Pean A, Pan W, Verfaillie CM. Identification of genes responsible for osteoblast differentiation from human mesodermal progenitor cells. *Proc Natl Acad Sci U S A* 2003; 100:3305–3310.
22. Stein GS, Lian JB, Van Wijnen AJ, et al. *Runx2* control of organization, assembly and activity of the regulatory machinery for skeletal gene expression. *Oncogene* 2004; 23:4315–4329.
23. Pfaffl MW. A new mathematical model for relative quantification in real-time RT-PCR. *Nucleic Acids Res* 2001; 29:e45.
24. Suzuki T, Higgins PJ, Crawford DR. Control selection for RNA quantitation. *Biotechniques* 2000; 29:332–337.
25. Thellin O, Zorzi W, Lakaye B, et al. Housekeeping genes as internal standards: use and limits. *J Biotechnol* 1999; 75:291–295.
26. Vandesompele J, De Preter K, Pattyn F, Poppe B, Van Roy N, De Paepe A, Speleman F. Accurate normalization of real-time quantitative RT-PCR data by geometric averaging of multiple internal control genes. *Genome Biol* 2002; 3:RESEARCH0034.
27. Reynolds ES. The use of lead citrate at high pH as an electron-opaque stain in electron microscopy. *J Cell Biol* 1963; 17:208–212.
28. Jemt T, Chai J, Harnett J, et al. A 5-year prospective multicenter follow-up report on overdentures supported by osseointegrated implants. *Int J Oral Maxillofac Implants* 1996; 11:291–298.
29. Nkenke E, Fenner M. Indications for immediate loading of implants and implant success. *Clin Oral Implants Res* 2006; 17(Suppl 2):19–34.
30. De Rouck T, Collys K, Cosyn J. Single-tooth replacement in the anterior maxilla by means of immediate implantation and provisionalization: a review. *Int J Oral Maxillofac Implants* 2008; 23:897–904.

31. Aghaloo TL, Moy PK. Which hard tissue augmentation techniques are the most successful in furnishing bony support for implant placement? *Int J Oral Maxillofac Implants* 2007; 22 (Suppl):49–70.
32. Simeone A, Acampora D, Pannese M, et al. Cloning and characterization of two members of the vertebrate *Dlx* gene family. *Proc Natl Acad Sci U S A* 1994; 91:2250–2254.
33. Klein MO, Grötz KA, Walter C, Wegener J, Wagner W, Al-Nawas B. Functional rehabilitation of mandibular continuity defects using autologous bone and dental implants – prognostic value of bone origin, radiation therapy and implant dimensions. *Eur Surg Res* 2009; 43:269–275.
34. Madrid C, Sanz M. What impact do systemically administered bisphosphonates have on oral implant therapy? A systematic review. *Clin Oral Implants Res* 2009; 20:87–95.
35. Laize V, Martel P, Viegas CS, Price PA, Cancela ML. Evolution of matrix and bone gamma-carboxyglutamic acid proteins in vertebrates. *J Biol Chem* 2005; 280:26659–26668.
36. Kinoshita S, Finnegan M, Bucholz RW, Mizuno K. Three-dimensional collagen gel culture promotes osteoblastic phenotype in bone marrow derived cells. *Kobe J Med Sci* 1999; 45:201–211.
37. Anderson HC, Sipe JB, Hessle L, Dhanyamraju R, Atti E, Camacho NP, Millan JL. Impaired calcification around matrix vesicles of growth plate and bone in alkaline phosphatase-deficient mice. *Am J Pathol* 2004; 164:841–847.
38. Hessle L, Johnson KA, Anderson HC, et al. Tissue-nonspecific alkaline phosphatase and plasma cell membrane glycoprotein-1 are central antagonistic regulators of bone mineralization. *Proc Natl Acad Sci U S A* 2002; 99:9445–9449.
39. Lian JB, Stein GS, Stein JL, van Wijnen AJ. Osteocalcin gene promoter: unlocking the secrets for regulation of osteoblast growth and differentiation. *J Cell Biochem Suppl* 1998; 30–31:62–72.
40. Lian JB, Javed A, Zaidi SK, et al. Regulatory controls for osteoblast growth and differentiation: role of Runx/Cbfa/AML factors. *Crit Rev Eukaryot Gene Expr* 2004; 14:1–41.
41. Knabe C, Howlett CR, Klar F, Zreiqat H. The effect of different titanium and hydroxyapatite-coated dental implant surfaces on phenotypic expression of human bone-derived cells. *J Biomed Mater Res A* 2004; 71:98–107.
42. Omar O, Lenneras M, Svensson S, et al. Integrin and chemokine receptor gene expression in implant-adherent cells during early osseointegration. *J Mater Sci Mater Med* 2010; 21:969–980.
43. Omar O, Svensson S, Zoric N, et al. In vivo gene expression in response to anodically oxidized versus machined titanium implants. *J Biomed Mater Res A* 2010; 92:1552–1566.
44. Aubin JE. Regulation of osteoblast formation and function. *Rev Endocr Metab Disord* 2001; 2:81–94.

Copyright of Clinical Implant Dentistry & Related Research is the property of Wiley-Blackwell and its content may not be copied or emailed to multiple sites or posted to a listserv without the copyright holder's express written permission. However, users may print, download, or email articles for individual use.